Grain-scale mechanical properties of lunar plagioclase and its simulant: Initial experimental findings and modeling implications.

D.M. Cole[1], L.A. Taylor[2], Y. Liu[2] and M.A. Hopkins[1]
[1] Engineer Research and Development Center – Cold Regions Research and Engineering Laboratory, Hanover NH
[2] Planetary Geosciences Institute, University of Tennessee – Knoxville.

ABSTRACT

Preparations for lunar missions involve the extensive use of simulants of lunar surface materials. Since many planned operations engage the mechanical properties of the regolith, it is of utmost importance to assure that the simulants adequately represent the engineering properties of actual lunar materials. To address this critical issue, we are conducting an experimental and modeling effort to quantify and compare the grain-scale properties of lunar materials and their simulants. Given the scarcity of lunar regolith for experimentation, we employ an approach to material characterization based on grain-to-grain contact experiments and use numerical modeling to extend the work to the engineering scale.

This paper describes the experimental methods, compares the contact properties of the materials under study, and discusses our on-going DEM modeling efforts. We present the results of an initial set of contact experiments conducted on the plagioclase component of the lunar simulant NU-LHT, and a number of highlands plagioclase grains obtained during the Apollo 17 mission. Our initial experiments indicate that the normal contact stiffness of the simulant plagioclase can be up to 2-3 times higher than the lunar highlands plagioclase, which appears to be primarily in the form of relatively weak micro-breccias. This difference is substantially lower for more intact lunar grains. Sliding contact experiments indicate that the shear stiffness at low force levels is close to the normal stiffness.

These preliminary experiments indicate that lunar highland simulants produced by simple crushing and grinding of plagioclase rock may not capture the actual strength of lunar highlands plagioclase. Continuous micro-meteorite space weathering of soil on the Moon can weaken grains considerably more than simple crushing/grinding. Additional experiments are in progress with plagioclase from contrasting maturity of soils, as well as with lunar rock plagioclase.

INTRODUCTION

The testing and development of equipment that will be deployed in planned lunar missions to the surface of the Moon will rely heavily on the use of simulants of the lunar regolith. Since these missions will involve many operations that engage the mechanical properties of the lunar regolith (e.g., surface mobility, drilling, excavation, and construction operations), it is of utmost importance to assure that the simulants adequately represent the engineering properties of actual lunar materials. An unusual aspect of this situation is the very limited supply of Apollo lunar material for use in experiments to validate the simulant properties. To address this issue, we are conducting grain-to-grain contact experiments on the components of the NU-LHT family of lunar simulants being produced by the USGS and comparing those to results of contact experiments on grains of Apollo highland lunar materials. Our

experimental methods are particularly well suited to the problem at hand because only a small number of representative grains is needed for characterization.

The goal of the experimental work is to characterize the grain-scale mechanical properties of the main mineralogical and morphological components of the lunar highlands materials and the associated simulants. This characterization serves two important needs. It will provide a quantitative assessment of how well the simulants represent the mechanical properties of the lunar regolith. In addition, it supports the development of a numerical simulation capability for virtual experimentation that will supplement more costly physical experimentation. Specifically, the information from our contact experiments supports the development of laws for the stiffness, frictional loss, and damage of grains of lunar material and simulants. These laws are subsequently incorporated into a discrete-element simulation of a triaxial cell to simulate the bulk engineering response of the material.

The work reported herein focuses on grain-scale testing and physical characterization of a number of plagioclase grains that are a component of the lunar simulant NU-LHT being produced by the USGS, and a number of plagioclase grains from an Apollo 17 soil, with a large highland component. We focus initially on plagioclase because of its relatively high abundance in the lunar highlands and the fact that it is readily identifiable. The results of normal and sliding contact experiments are presented, with emphasis on contact stiffness and frictional loss in these two important modes of grain interaction. Quantities of the main components of NU-LHT were kindly provided by the USGS, and the grains employed in the present experiments were from a coarse sieve fraction (between #35 and #100 sieves) and were somewhat larger than our lunar grains.

In addition to a comparison of the micromechanical properties of the lunar grains and the simulants, some attention is paid to their general grain size and shape characteristics, and the incorporation of the contact laws and shape characteristics of the grains into our DEM triaxial simulation is discussed.

PHYSICAL CHARACTERISTICS AND SPECIMEN PREPARATION

The plagioclase grain characterizations are based on optical and scanning electron microscopy (see Park et al., 2008 and Liu et al., 2008). Great care was taken to select representative grains, identify a contact patch of interest on each grain, and mount the grains with the contact patch properly oriented. Specimens were mounted on stainless steel pins (described in the following section) and orthogonal sets of side-view images of each grain were obtained to quantify the radius of curvature and roughness of the contact area. Care was taken to obtain high-contrast side-view images of the grains, with an image resolution of approximately 1 pixel μm^{-1}. Images were obtained before and after the contact experiment to provide quantitative information on changes in the local radius of curvature and roughness due to damage. Figures 1 and 2 show representative SEM images of the tested grains.

An eventual goal of our modeling effort is to quantify curvature and roughness effects on contact behavior, and our methods for detailed characterization of these quantities are under development. We employed a quantitative image processor (Image Pro Plus) to obtain a digital profile from the two orthogonal views of each grain surface for analysis. Figure 3 shows a typical side-view SEM image of a lunar

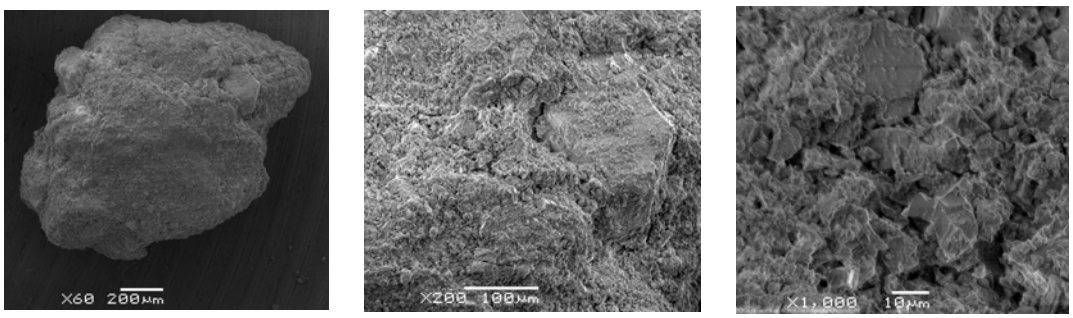

Figure 1. SEM micrographs of lunar plagioclase grain 4 at increasing levels of magnification (L to R) as indicated. Note the highly fissured nature of this material.

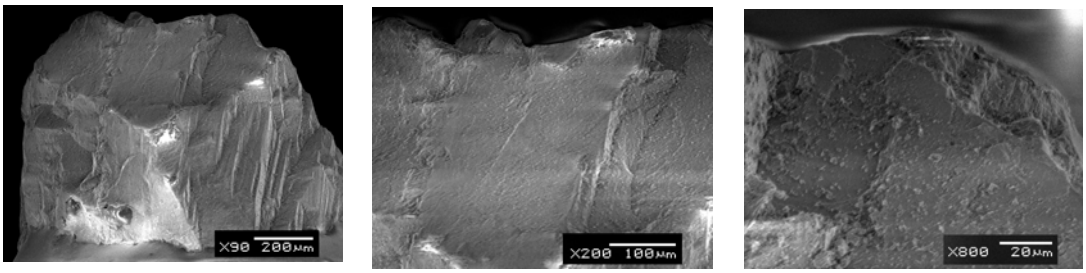

Figure 2. SEM micrographs of USGS plagioclase grain 9 at increasing levels of magnification (L to R) as indicated. Note that this material appears to be more robust than the lunar plagioclase as it lacks the extensive network of cracks and fissures evident in Figure 1.

highlands plagioclase grain along with the profile obtained by the image processor. The radius of curvature (RoC) values reported in Table 1 were obtained from a best fit (least-squared error) analysis of a circular arc through selected points along the grain profile. The region of contact for the mounted grains was generally obvious, and the profile points in that region were selected for this analysis. Table 2 details general grain size and shape statistics obtained from the image processor.

Table 1. Average radius of curvature measurements.

Material	Grain No.	Average RoC (mm)
Lunar highlands plagioclase	1	0.542
	2	0.292
	3	0.200
	4	0.537
	5	0.616
	6	0.308
	7	0.270
	8	0.046
USGS Plagioclase	1	0.453
	2	0.519
	3	0.152
	4	0.373
	5	1.158
	6	0.639

It was abundantly clear upon handling that the lunar grains were of a friable nature, and we attribute this to the presence of micro-fissures that are evident in the images of the

Table 2. Grain statistics.

Average quantity	Lunar highlands plagioclase	USGS Plagioclase
Mean diameter (mm)	0.856 ± 0.232	1.831 ± 0.365
Aspect ratio	1.472 ± 0.427	1.468 ± 0.278
Major axis (mm)	1.052 ± 0.397	2.229 ± 0.507
Minor axis (mm)	0.717 ± 0.162	1.538 ± 0.309
Roundness	1.48 ± 0.174	1.520 ± 0.153

lunar plagioclase (see Fig. 1). Clearly the lunar grains are not fresh pieces of plagioclase.

We note that the highlands plagioclase grains and micro-breccias examined here are typical of lunar highlands soils, and it is presumed that the extensive micro-meteorite space weathering and gardening to which they are exposed is responsible for their relative mechanical weakness. The simulant plagioclase (see Fig. 2), in contrast, appeared much more robust and relatively free of serious flaws of type evident in the lunar plagioclase. As discussed below, we feel that this fundamental difference between the two materials explains the relative weakness of the lunar material.

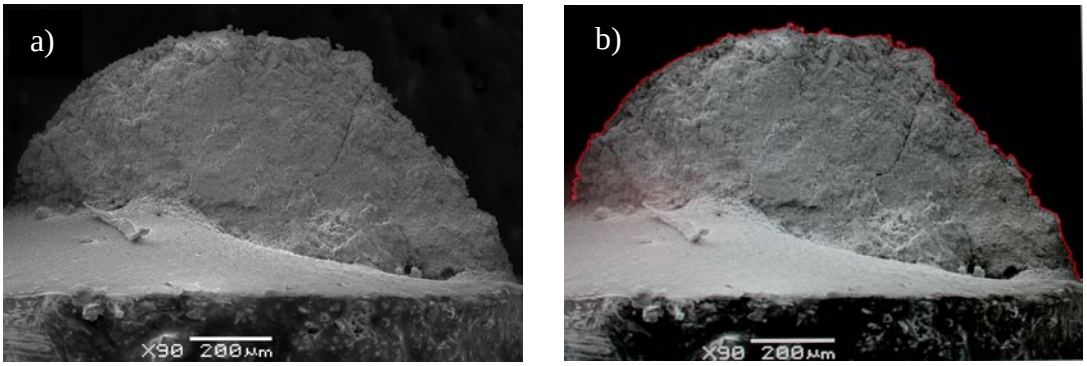

Figure 3. SEM micrographs of lunar highlands plagioclase grain 4 mounted for a normal contact experiment. a) High-contrast side view of grain prior to testing. b) Outline of grain profile as obtained with a quantitative image processor. The scaled outline was used for curvature and roughness analysis. Orthogonal side views at various magnifications were obtained on each grain prior to and after the contact experiments.

CONTACT EXPERIMENTS

The equipment employed in the contact experiments has been described in detail elsewhere (Cole and Peters, 2007, 2008), so only a brief description is provided here. The normal- and shear-contact experiments were conducted on a closed-loop, electro-mechanical testing system operated in load control. The system employs analog motion control which generates minimal EM interference with the system's extremely sensitive load and displacement transducers. When integrated into the test system, the load transducers reliably measured to 0.01 N and the laser-based deformation transducer had a resolution of 100 nm.

For the normal-contact experiments, the grains were brought into nominal no-load contact, and a compressive load was applied either according to a haversine function or a linearly increasing ramp to a specific force level or contact failure, depending on the goal of the particular experiment. The sliding-contact experiments were performed with the same control system and actuator as the normal-contact experiments, but with following modifications to the fixture. The specimens were oriented vertically with the lower specimen attached to the loading frame and the upper specimen attached to the actuator. A dead load system applied a constant normal force to the pin upon which the upper grain was mounted.

Cyclic haversine loading was primarily employed in the normal-contact experiments, with the peak normal force increasing from approximately 0.1 to 10 N, in increments ranging from 0.1 to 2 N. A similar sequence of increasing shear forces was applied to the sliding contacts except that the waveform for the shear cycles was a zero mean-stress sine wave, and that sequence was repeated under several levels of normal force ranging from 2 to 10 N for the simulant grains and for 2 and 4 N for the lunar material. Five to 10 cycles were applied at each force level, followed by a brief recovery period. The normal force was kept low for the lunar grains to avoid catastrophic damage. We examined frequency effects over the range of 2×10^{-2} to 3 Hz in a limited number of cases, to make a preliminary assessment of the extent to which rate effects should be of concern in the subject materials.

The sequence of normal force for the sliding contact experiments started at 10 N and decreased to 2 N, typically in 2 N increments. The intent of starting at the highest normal load was to avoid potential complications if the higher normal loads were to cause contact damage during the course of the experiment. With this approach, any minor contact damage imparted by the maximum normal force would be imparted at the start of the experiment and affect the results equally.

The lunar grains were problematic in the shear experiments as a result of their relative weakness. They were assessed to be incapable of sustaining the 10 N maximum normal load applied to the simulant grains without suffering excessive damage, so our initial experiments were restricted to normal forces of 2 and 4 N. In the shear experiments, the maximum shear force applied to a contact decreased with the normal force. This was required to avoid macroscopic sliding which could relocate the contact and thereby alter the response.

The majority of the experiments reported below involve cyclic loading because this approach provides a great amount of constitutive information without imparting significant damage to the contacts, and allows for a relatively large number of stress states to be examined for a given grain pair. Ramp loading (a monotonically increasing normal or shear force applied until macroscopic sliding occurs) provides useful information, but typically results in contact damage for nominally rough surfaces. That type of experiment, however, establishes important quantities such as the crushing strength of the contact under normal loading and the macroscopic coefficient of friction under shear loading. As a consequence of these considerations, we have conducted several macroscopic sliding experiments on the simulant grains, but none to date on the lunar grains.

The methods of analysis of the contact data have been described elsewhere (Cole and Peters, 2007, 2008). Briefly, the raw data points are smoothed by a piece-wise

regression routine that does not produce phase shift. The reported values of stiffness (slope of the force-deformation curve between the maximum and minimum levels of applied force), hysteresis-loop width and area, and internal friction are averages of the second and subsequent loading cycles applied under the specified loading conditions. The first cycle is omitted from the analysis to avoid transient effects.

RESULTS AND DISCUSSION

Experimental. Figures 4 and 5 show representative results for stiffness and internal friction, respectively, from the normal-contact experiments on the lunar highlands and simulant plagioclase grains. The trends for normal stiffness to increase and internal friction to decrease with increasing normal stress is in keeping with recent findings on other materials (Cole, 2008; Cole and Peters, 2008). It is apparent from our initial results that the normal stiffness of the simulant plagioclase can be 2-3 times higher than the lunar highlands plagioclase, which appears to be primarily in the form of relatively weak micro-breccias. This difference is substantially lower for more intact lunar grains, which were in a distinct minority of the 8 grains of lunar material employed in the present set of experiments. The apparent internal friction of the lunar micro-breccias observed under cyclic normal loading can be up to two times higher than the simulant.

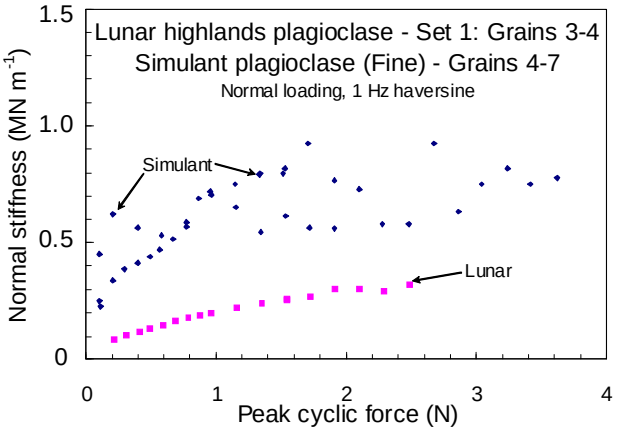

Figure 4. Normal stiffness vs. peak cyclic force for lunar and simulant grains as indicated.

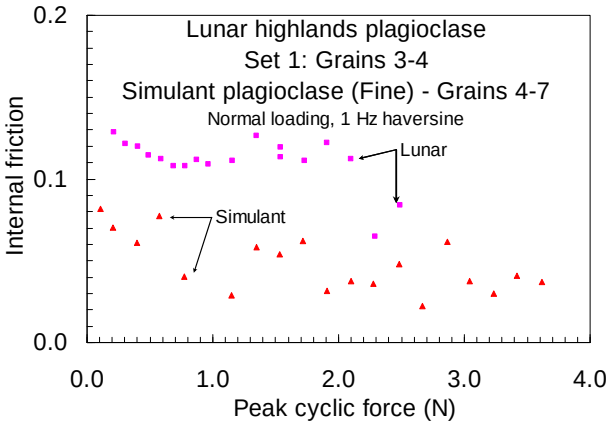

Figure 5. Internal friction vs. peak cyclic force for the lunar and simulant grains as indicated.

With reference to Figure 6, a limited number of shear experiments were conducted on the lunar grain pair 6-8 to complement the more extensive set of normal-loading experiments. As theory suggests (Mindlin and Deresiewicz, 1953), the shear stiffness for both materials is approximately equal to the normal stiffness under similar normal loads. Under a normal force of 2 N, the shear stiffness of the lunar grains was found to be 0.28 MN m^{-1}, in excellent agreement with the normal stiffness of 0.3 MN m^{-1} found at a normal force of 2 N. The simulant grains showed a similar relationship although the stiffness values are considerably higher. Figure 6 illustrates the trends for shear stiffness to increase with normal force and decrease with shear force amplitude, in agreement with our observations on other geologic granular media as cited above.

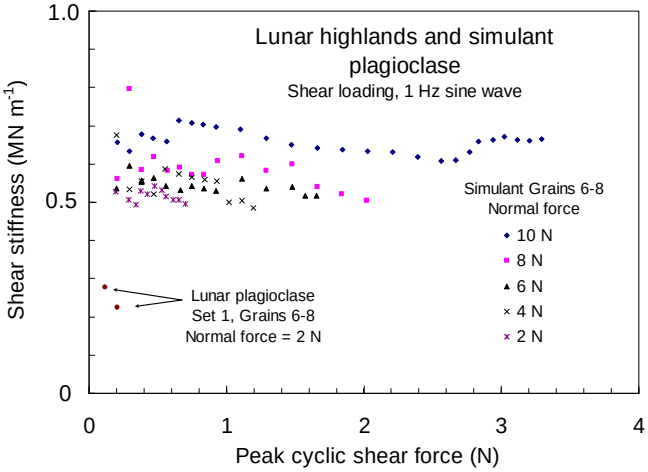

Figure 6. Shear stiffness vs. peak cyclic shear force under the normal forces indicated.

Figure 7 shows a log-log plot of the peak force- peak deformation data for several lunar and simulant grain pairs. The normal force-displacement data for the simulant suggests a linear relationship at lower forces with a shift to a Hertzian 3/2 power relationship at higher forces, with a nominal breakpoint near 1 N, although this is highly variable. The lunar grain pairs give some evidence of a linear relationship between normal force and displacement below 1 N (e.g., grain pairs 2-8 and 5-7), and a higher-power relationship at higher force levels (grain pair 3-4). The variations from Hertzian behavior are believed to be rooted in surface roughness. Our analysis to date suggests that the radius of curvature of the grains correlates strongly with contact behavior only for relatively smooth surfaces (Cole and Peters, 2008) that display Hertzian behavior. The normal-contact behavior of rough surfaces, on the other hand, does not display a clear-cut dependence on the radius of curvature in the contact region. This is a matter of on-going interest.

Our approach to modeling contact behavior is to develop separate expressions for the nominally elastic and inelastic component of deformation. We quantify the inelastic component through an analysis of the hysteresis observed under cyclic loading. Although hysteresis-loop width gives a direct measure of inelastic deformation, it is frequently difficult to quantify – particularly when deformations are small. Hysteresis-loop area frequently proves to be a more reliable quantity to measure, since it averages out the scatter associated with point-to-point variations over a loading cycle. Figure 8 shows a log-log plot of hysteresis-loop area vs. peak cyclic force for the lunar and simulant grains, with a 2:1 slope indicated. Although several of the simulant grains show some dispersion at forces above approximately 2 N, the data overall display a tendency to follow a 2nd power dependency of loop area on peak force. Since the

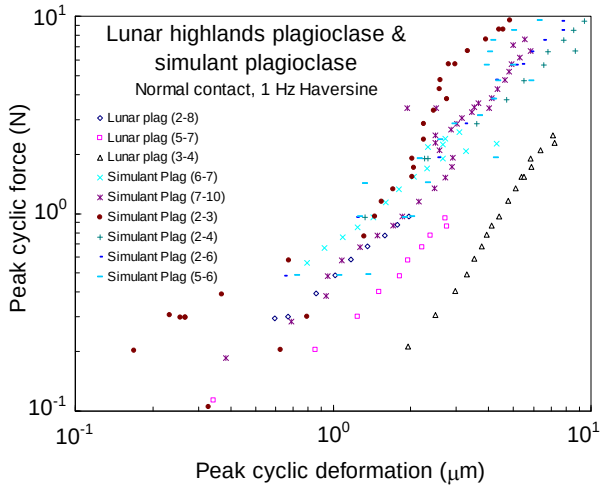

Figure 7 Peak cyclic force vs. peak cyclic deformation for lunar and simulant grains.

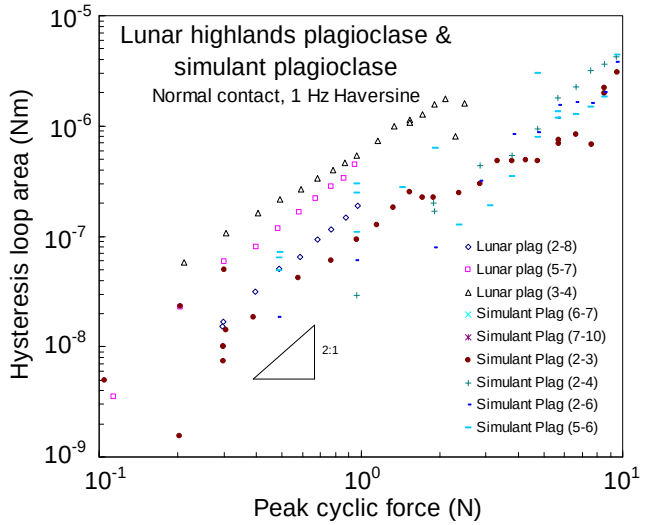

Figure 8. Hysteresis-loop area vs. peak cyclic force or lunar and simulant plagioclase.

loop area is proportional to the loop width and peak force, this 2nd power dependence of the loop area indicates a linear relationship between the loop width (a direct measure of the inelastic deformation) and the peak force. This matter is considered further below.

With regard to frequency effects on normal contact behavior, Figure 9 shows the results for lunar plagioclase grains 5 and 7. Although dry granular media generally do not display a pronounced frequency effect, the indicated range in frequency shows a dispersion in stiffness and internal friction. Another grain pair of lunar plagioclase displayed a similar trend over this frequency range, although the stiffness was some 65% higher and the associated internal friction was 48% lower. Evidence of a frequency effect for the simulant plagioclase grains was inconsistent in the grain pairs examined as of this writing. The observation of a frequency effect in the lunar plagioclase (which has a substantially lower stiffness and higher internal friction than the simulant) suggests that the underlying loss mechanism is related to the lunar material's highly flawed microstructure.

The overall goal of the work is to develop contact laws – based on the results of the grain-scale experiments – for each of the components of NU-LHT and implement these laws in discrete element model to simulate the engineering properties of the aggregate material. This approach develops a direct link between the contact properties of the constituent grains and the bulk engineering properties, as demonstrated in Uthus et al. (2008). As a consequence of this linkage, there are concerns about the ability of the plagioclase component of the NU-LHT simulant to adequately reproduce the mechanical properties of the lunar highlands plagioclase.

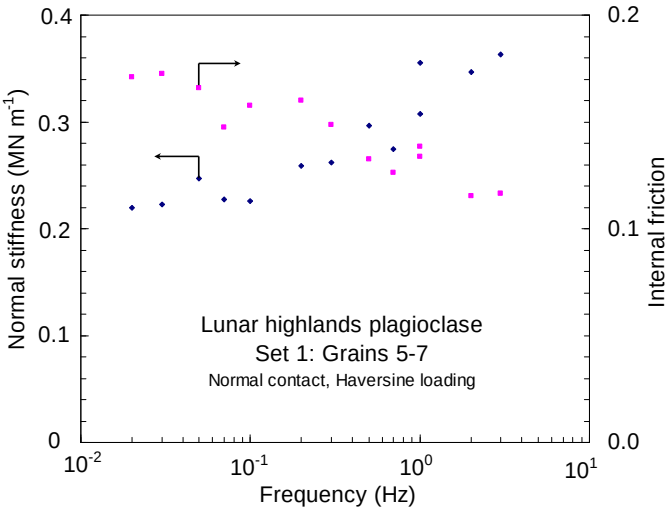

Figure 9. Normal stiffness and internal friction vs. cyclic loading frequency for lunar plagioclase grains.

As of this writing, we are planning to conduct experiments on plagioclase grains that were harvested from rock specimens and

appear to have suffered less degradation than the grains examined thus far. Those results will offer some insight regarding the extent to which exposure to the lunar environment alters the grain-scale mechanical properties of plagioclase. In addition to plagioclase, our on-going comparison between the contact properties of lunar material and simulants is extending to other components of the lunar regolith, with the goal of establishing how their properties may differ from simulants of the appropriate composition but which have not been exposed to the lunar environment.

SUMMARY AND CONCLUSIONS

We have conducted a series of normal- and shear-contact experiments on grain pairs of lunar highlands plagioclase and grains of plagioclase being produced for use in the NU-LHT family of simulants. The work involved the use of SEM and quantitative image processing to characterize the size, shape and surface morphology of the individual grains, and grain-scale micromechanical testing methods to quantify the normal and shear contact behavior. The following conclusions are drawn based on the work described above:

1. SEM micrographs indicate that the lunar plagioclase grains are generally fissured and consist to some extent of micro-breccia, whereas the simulant grains were appreciably more robust and generally free of major microstructural flaws.
2. The normal contact properties of the lunar highlands plagioclase and simulant plagioclase grains studied here vary substantially. Under the prevailing conditions:

    a. The normal contact stiffness of the simulant ranged from ≈ 0.2 to 0.9 MN m^{-1}, compared to a range of 0.1 to 0.44 MN m^{-1} for the lunar grains.

    b. For normal loading conditions that produced internal friction values of 0.02 to 0.08 for the simulant grains, values in the range of 0.11 to 0.13 were found for the lunar grains.

3. The shear-contact properties of the lunar highlands and simulant plagioclase grains varied substantially. Under a normal load that produced shear stiffness of ≈ 0.5 MN m^{-1}, the lunar material exhibited shear stiffness in the range of 0.2 to 0.3 MN m^{-1}.

ACKNOWLEDGEMENTS

This work was supported by NASA's Lunar Advanced Science and Exploration Research program (LASER07). We thank Dr. Steve Wilson and Douglas Stoeser of the USGS for helpful discussions and providing us with samples of the NU-LHT components.

REFERENCES

Cole, D.M. and J.F. Peters (2008) Grain-scale mechanics of geologic materials and lunar simulants under normal loading. Granular Matter, Vol. 10, pp. 171-185, DOI: 10.1007/s10035-007-0066-y

Cole, D.M. (2008). "Stiffness and friction of normal and sliding contacts of geologic materials", *Proceedings of ASCE Earth & Space 2008*, Eds., R. B. Malla, W. K. Biniendan and A. K. Maji, March, 2008.

Cole, D.M. and J.F. Peters (2007) A physically based approach to granular media mechanics: Grain-scale experiments, initial results and implications to

numerical modeling. Granular Matter, Vol. 9, No. 5, pp. 309-321, DOI: 10.1007/s10035-007-0046-2

Mindlin, R.D. and H. Deresiewicz (1953) Elastic spheres in contact under varying oblique forces. ASME J. Appl. Mech., Vol. 20, pp. 327-344.

Park, J., Y. Liu, K.D. Kihm, and L.A. Taylor (2008) Characterization of Lunar Dust for Toxicological Studies. I: Particle Size Distribution. J. Aerospace Eng., Vol. 21, No. 4, pp. 266-271. DOI: 10.1061/(ASCE)0893-1321(2008)21:4(266)

Liu, Y., J. Park, D. Schnare, E. Hill and L.A. Taylor (2008) Characterization of Lunar Dust for Toxicological Studies. II: Texture and Shape Characteristics. J. Aerospace Eng., Vol. 21, No. 4, pp. 272-279. DOI: 10.1061/(ASCE)0893-1321(2008)21:4(272)

Uthus, L., M.A. Hopkins and I. Horvli (2008) Discrete element modelling of the resilient behaviour of unbound granular aggregates. Intl. J. Pavement Eng., Vol. 9, No. 6, pp. 387-395.